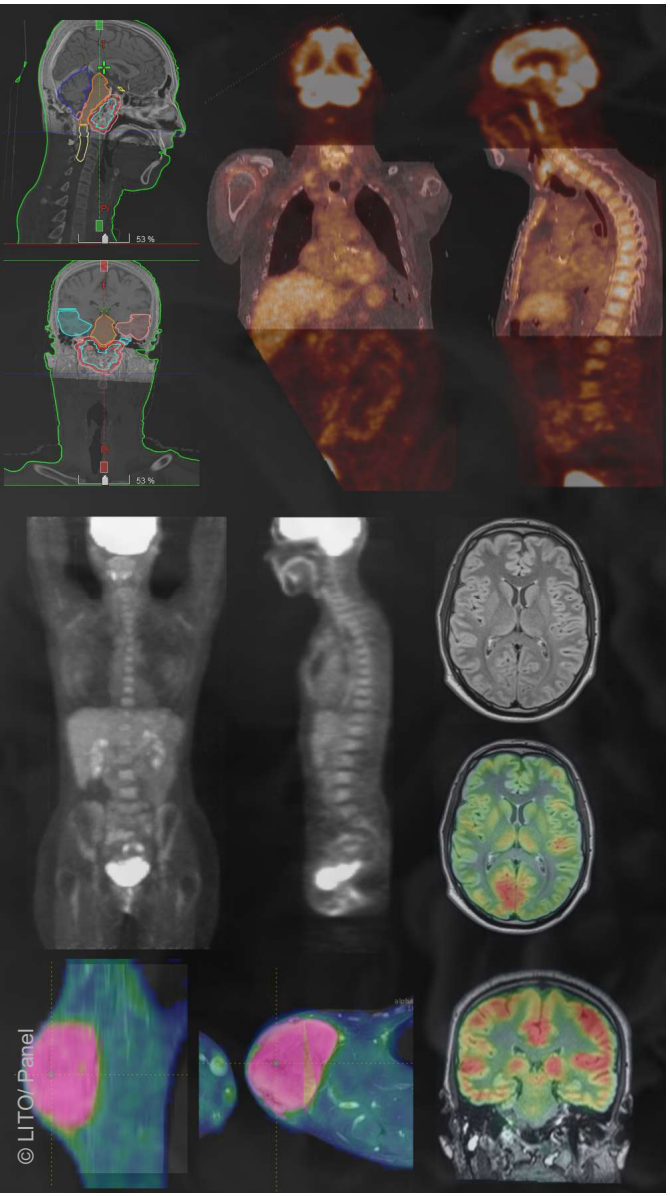

Retour SNMMI 2021

09/09/2021

A méditer …

June 11-15

SNMMI 2021 *Virtual* ANNUAL MEETING

*"Innovation is not always a new device or technology, but simply finding a **new/novel** way to use an existing technology."*

A Tribute to Sanjiv (Sam) Gambhir

The molecular imaging community has lost a brilliant scientist and visionary, but, more importantly, a genuinely empathetic and caring individual and a friend. We are profoundly grateful for his vast contributions to science, medicine and humanity. Our thoughts are with his wife, Aruna, and the extended Gambhir family.

Comment utiliser au maximum les informations disponibles ?

SUVmax described in FDG PET-CT reports can provide information of lesion location: an investigation of real-world data

Kenji Hirata, Yuko Uchiyama, Shiro Watanabe, Sho Furuya and Kohsuke Kudo

Journal of Nuclear Medicine May 2021, 62 (supplement 1) 1194;

Background

- FDG-PET/CT reports often describe the maximum standardized uptake value (SUVmax) to express the intensity of FDG uptake.
- SUVmax is written with various decimal places (DP):
  - 1st DP 3.1 (indicating 3.05 ~ 3.15)
  - 2nd DP 3.14 (indicating 3.135 ~ 3.145)
  - 3rd DP 3.142 (indicating 3.1415 ~ 3.1425)
- If SUVmax is written in higher decimal places, it could have information for identifying the lesion location in the image, because there should be limited number of voxels that satisfy the SUVmax description.
- We published preliminary data (Hirata et al. Front. Med. 2021), demonstrating that 97.8% of lesions could be uniquely identified under the condition that 1) SUVmax > 5, 2) SUVmax is described with 3rd DP, and 3) local maximum restriction is applied.
- However, since the ***real-word*** PET/CT reports were not used in the previous study, it has not been clear how well the method works for the actual reports.
- **Aim of the study**: To investigate the FDG-PET/CT reports in our institute retrospectively to clarify whether SUVmax in the reports can be used as an identifier for lesions.

Question: Is 1:1 correspondence possible between report and image using SUVmax?

PET/CT report

An uptake mass (SUVmax=5.093) is observed in the mediastinum, indicating paratracheal lymph node metastasis....

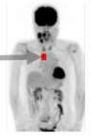

Conclusion

SUVmax strings in the FDG-PET/CT reports could be used for lesion localization. Further algorithms will improve the performance.

Methods

- Retrospective single-center study
- Hokkaido University Hospital IRB approval (No.017-0454)
- Informed consent waived
- Study period: a total of 20 working days from the periods of January 11-20, 2017, May 11-20, 2014, and September 11-20, 2011.
- A total of 230 FDG-PET/CT examinations were investigated.
- **Regular expression** was used to extract the strings that possibly represented SUVmax in the PET/CT reports, a regular expression formula ¥d+(¥. |.)¥D+ was used to extract float numbers (e.g., 3.14).
- **Post-processing** after the regular expression process, the followings were excluded:
  - containing 2 period characters (e.g., 2020.11.6) (date string)
  - "MBq" followed (e.g., 234.5MBq) (dosage string)
  - "Previous study" preceded within 4 characters.
- **Radiologist's evaluation:** an experienced nuclear medicine physician evaluated all the SUVmax strings to determine true SUVmax or not.
- **The algorithm for lesion localization based on SUVmax string**
  - All voxels in the whole-body image were searched to extract the voxels having a nearby value.
  - In case of SUVmax = '3.14', voxels of 3.135≤x<3.145 were extracted.
  - Local maximum restriction: only the voxel that was local maximum within the 5×5×5 voxel space.
  - In case only 1 voxel satisfied the criteria, it was defined as *successful*.
  - In the example case, the voxel 8.1 is local maximum, but 7.1 is not.
- Software environments
  - Visual Studio 2019 version 16.7.5
  - C#8 & .NET Core 3.1
  - Metavol
  - Fellow Oak DICOM
  - Math.NET

Example case (number = SUV)

7.9	6.1	8.0	7.7
6.5	8.1	5.5	6.5
7.4	5.8	7.1	6.2
7.5	5.9	6.9	5.8

Visual Studio Fellow Oak DICOM metavol

Disclosures The authors have no conflicts of interest with regard to this research.

Funding This work was supported by JST COI Grant Number JPMJCE1301 (H31W09) and JSPS KAKENHI Grant Number JP20K08015.

Results

Case 1: Recurrence of rectal cancer. The PET/CT report indicated following lesions:
- Right inguinal (SUVmax=6.482)
- Pancreatic body (9.648)
- Right spermatic cord (4.546)

SUVmax was written with 3rd DP.
All the lesions were appropriately identified using the proposal method

6.482 9.648 4.546

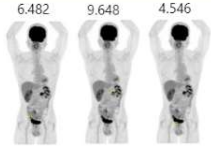

Case 2: Lung cancer. The PET/CT report indicated following lesions:
- Right upper lobe of the lung (SUVmax=18.2)
- Left adrenal grand (6.3) *Detection Failed*
- Para-aortic node (6.6)

SUVmax was written with 1st DP.
Two SUVmax strings were appropriately associatec to the voxel, but the other one was not.
'SUVmax=6.3' corresponded to 3 different voxels, among which one (arrow) was the true lesion.

18.2 6.3 6.6

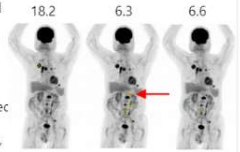

- 435 SUVmax strings were automatically detected in 230 PET/CT exams.
- After physician's inspection, 333 strings were judged as true SUVmax strings (i.e., 102 strings were excluded).
- The success rate varied depending on (1) the SUVmax range of the lesion and (2) the precision of the SUVmax string.
- In case 20≤SUVmax, 91% cases were successful, whereas only 13% cases were successful in case SUVmax<2.
- When SUVmax was written with 1st decimal places (DP), only 29% cases were successful. In contrast, 91% cases were successful when written with 3rd DP.

Table. Success rate by SUVmax range and decimal places (DP)

SUVmax	1st DP	2nd DP	3rd DP	Total
x<2	0/11 (0%)	NA	2/4 (50%)	2/15 (13%)
2≤x<5	13/114 (11%)	0/1 (0%)	32/35 (91%)	45/150 (30%)
5≤x<10	26/71 (37%)	4/6 (67%)	15/17 (88%)	45/94 (48%)
10≤x<20	27/44 (61%)	NA	19/19 (100%)	46/63 (73%)
20≤x	5/6 (83%)	NA	5/5 (100%)	10/11 (91%)
Total	71/246 (29%)	4/7 (57%)	73 (91%)	148/333 (44%)

Comment utiliser au maximum les informations disponibles ?

SUVmax described in FDG PET-CT reports can provide information of lesion location: an investigation of real-world data

Kenji Hirata, Yuko Uchiyama, Shiro Watanabe, Sho Furuya and Kohsuke Kudo

Journal of Nuclear Medicine May 2021, 62 (supplement 1) 1194;

Background

- FDG-PET/CT reports often describe the maximum standardized uptake value (SUVmax) to express the intensity of FDG uptake.
- SUVmax is written with various decimal places (DP):
  - 1st DP 3.1 (indicating 3.05 ~ 3.15)
  - 2nd DP 3.14 (indicating 3.135 ~ 3.145)
  - 3rd DP 3.142 (indicating 3.1415 ~ 3.1425)
- If SUVmax is written in higher decimal places, it could have information for identifying the lesion location in the image, because there should be limited number of voxels that satisfy the SUVmax description.
- We published preliminary data (Hirata et al. Front. Med. 2021), demonstrating that 97.8% of lesions could be uniquely identified under the condition that 1) SUVmax > 5, 2) SUVmax is described with 3rd DP, and 3) local maximum restriction is applied.
- However, since the ***real-word*** PET/CT reports were not used in the previous study, it has not been clear how well the method works for the actual reports.
- **Aim of the study**: To investigate the FDG-PET/CT reports in our institute retrospectively to clarify whether SUVmax in the reports can be used as an identifier for lesions.

Question: Is 1:1 correspondence possible between report and image using SUVmax?

PET/CT report

An uptake mass (SUVmax=5.093) is observed in the mediastinum, indicating paratracheal lymph node metastasis....

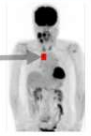

Conclusion

SUVmax strings in the FDG-PET/CT reports could be used for lesion localization. Further algorithms will improve the performance.

Methods

- Retrospective single-center study
- Hokkaido University Hospital IRB approval (No.017-0454)
- Informed consent waived
- Study period: a total of 20 working days from the periods of January 11-20, 2017, May 11-20, 2014, and September 11-20, 2011.
- A total of 230 FDG-PET/CT examinations were investigated.
- **Regular expression** was used to extract the strings that possibly represented SUVmax in the PET/CT reports, a regular expression formula ¥d+(¥. |.)¥D+ was used to extract float numbers (e.g., 3.14).
- **Post-processing** after the regular expression process, the followings were excluded:
  - containing 2 period characters (e.g., 2020.11.6) (date string)
  - "MBq" followed (e.g., 234.5MBq) (dosage string)
  - "Previous study" preceded within 4 characters.
- **Radiologist's evaluation:** an experienced nuclear medicine physician evaluated all the SUVmax strings to determine true SUVmax or not.
- **The algorithm for lesion localization based on SUVmax string**
  - All voxels in the whole-body image were searched to extract the voxels having a nearby value.
  - In case of SUVmax = '3.14', voxels of 3.135≤x<3.145 were extracted.
  - Local maximum restriction: only the voxel that was local maximum within the 5×5×5 voxel space.
  - In case only 1 voxel satisfied the criteria, it was defined as *successful*.
  - In the example case, the voxel 8.1 is local maximum, but 7.1 is not.
- Software environments
  - Visual Studio 2019 version 16.7.5
  - C#8 & .NET Core 3.1
  - Metavol
  - Fellow Oak DICOM
  - Math.NET

Visual Studio Fellow Oak DICOM metavol

Example case (number = SUV)

7.9	6.1	8.0	7.7
6.5	8.1	5.5	6.5
7.4	5.8	7.1	6.2
7.5	5.9	6.9	5.8

Disclosures The authors have no conflicts of interest with regard to this research.

Funding This work was supported by JST COI Grant Number JPMJCE1301 (H31W09) and JSPS KAKENHI Grant Number JP20K08015.

Results

Case 1: Recurrence of rectal cancer. The PET/CT report indicated following lesions:
- Right inguinal (SUVmax=6.482)
- Pancreatic body (9.648)
- Right spermatic cord (4.546)

SUVmax was written with 3rd DP.
All the lesions were appropriately identified using the proposal method

6.482 9.648 4.546

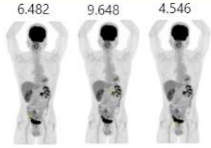

Case 2: Lung cancer. The PET/CT report indicated following lesions:
- Right upper lobe of the lung (SUVmax=18.2)
- Left adrenal grand (6.3) *Detection Failed*
- Para-aortic node (6.6)

SUVmax was written with 1st DP.
Two SUVmax strings were appropriately associatec to the voxel, but the other one was not.
'SUVmax=6.3' corresponded to 3 different voxels, among which one (arrow) was the true lesion.

18.2 6.3 6.6

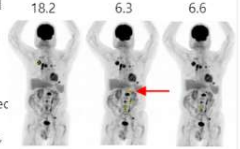

- 435 SUVmax strings were automatically detected in 230 PET/CT exams.
- After physician's inspection, 333 strings were judged as true SUVmax strings (i.e., 102 strings were excluded).
- The success rate varied depending on (1) the SUVmax range of the lesion and (2) the precision of the SUVmax string.
- In case 20≤SUVmax, 91% cases were successful, whereas only 13% cases were successful in case SUVmax<2.
- When SUVmax was written with 1st decimal places (DP), only 29% cases were successful. In contrast, 91% cases were successful when written with 3rd DP.

Table. Success rate by SUVmax range and decimal places (DP)

SUVmax	1st DP	2nd DP	3rd DP	Total
x<2	0/11 (0%)	NA	2/4 (50%)	2/15 (13%)
2≤x<5	13/114 (11%)	0/1 (0%)	32/35 (91%)	45/150 (30%)
5≤x<10	26/71 (37%)	4/6 (67%)	15/17 (88%)	45/94 (48%)
10≤x<20	27/44 (61%)	NA	19/19 (100%)	46/63 (73%)
20≤x	5/6 (83%)	NA	5/5 (100%)	10/11 (91%)
Total	71/246 (29%)	4/7 (57%)	73 (91%)	148/333 (44%)

Infos +++
à extraire des CR pour nos études rétrospectives!

Quantification TMTV automatique

Improved clinical feasibility of total tumor burden quantification on 68Ga-PSMA-11 PET/CT through deep learning auto-segmentation of organs for automatic physiological uptake removal.

Remy Niman, Peter Wilson, Louise Emmett, Sarennya Pathmanandavel and Aaron Nelson

Journal of Nuclear Medicine May 2021, 62 (supplement 1) 1327;

Objectives: The utility of total tumor burden (TTB) quantification of 68Ga-PSMA-11 PET/CT for treatment response prediction has been shown (Schmidkonz C et al, 2018; Schmuck S et al, 2017). The main challenges preventing semi-automatic lesion segmentation from being used in clinical practice are the time required to segment each lesion for patients with high tumor burden and to remove the physiologic uptake captured when using whole body automatic segmentation methods based on SUV thresholds. The objective of this study is to evaluate the use of a deep learning algorithm to create CT-based organ VOIs with a whole body segmentation tool to remove the majority of the PET physiological uptake automatically.

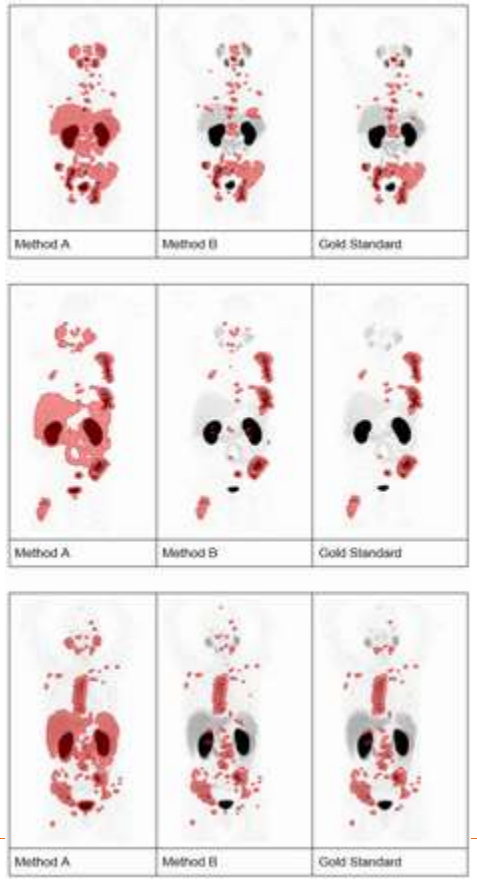

Pour plusieurs traceurs
(pas que FDG !)
→ Fixations physiologiques ≠

Quantification TMTV automatique

Methods: 78 68Ga-PSMA-11 PET/CT studies were analyzed from the LuPIN trial dataset. Gold Standard (GS) TTB VOIs were created using a semi-automatic workflow with an SUV threshold of 3 followed by manual removal of physiological uptake by a credentialed nuclear medicine physician (Crumbaker M et al, 2020). During the GS TTB VOI creation, some regions below 3 SUV were added. Since the liver background activity was typically higher than 3 SUV, a gradient-based method was used to segment liver lesions. 2 whole body segmentation methods were used for evaluation: Method A and Method B. Method A used an SUV threshold of 3 to automatically segment the lesions within the whole body. Lesions of any size were kept within the bone VOI; lesions within the rest of the body were removed if they were less than 0.2ml in size. Method B consisted of lesions from Method A with additional logic applied for removing physiologic uptake. First, a deep learning segmentation method was used to create CT-based organ VOIs for areas of physiological uptake (submandibular glands, parotid glands, bowel, kidneys, bladder) and the liver (NM Cole et al, 2020; A Kruzer et al, 2020; D Mirando, 2020). An atlas-based method was used for the spleen (a physiological uptake VOI) and the pelvic lymph nodes. An HU-based threshold segmentation method was used to create a bone VOI. Areas of increased 68Ga-PSMA-11 activity within the normal organ VOIs were removed automatically. The pelvic lymph node and bone VOIs were used in conjunction with the organ VOIs to prevent activity found in these areas from being removed. Lesions within the liver used a separate SUV threshold of 2 times the SUV mean of an automatically placed 3cm spherical liver reference region.

Methods

- 78 ^{68}Ga-PSMA-11 PET/CT studies were analyzed from the LuPIN trial dataset[3].
- **Ground Truth segmentation[3]:**
  - Expert nuclear medicine physician used a 3 SUV threshold value and gradient-based segmentation tool (liver lesions only) to segment lesions and manually removed physiological uptake.
- **Proposed segmentation:**
  - Automatic whole body PET segmentation method using a 3 SUV threshold value followed by physiological uptake removal using organs segmented based on the CT.

Organ	Type of Uptake	Segmentation Method	Use in Physiological Uptake Removal Algorithm
Submandibular Glands	Physiological	Deep Learning Algorithm	Removed
Parotid Glands	Physiological	Deep Learning Algorithm	Removed
Bowel	Physiological	Deep Learning Algorithm	Removed
Kidneys	Physiological	Deep Learning Algorithm	Removed
Bladder	Physiological	Deep Learning Algorithm	Removed
Spleen	Physiological	Atlas	Removed
Liver	Possible Lesions	Deep Learning Algorithm	Uptake Kept
Pelvic Lymph Nodes	Possible Lesions	Atlas	Uptake Kept
Bone	Possible Lesions	HU-based thresholding	Uptake Kept

TABLE 1: Various CT organs were segmented in order to remove physiological uptake. Automatically segmented uptake that overlapped the physiological uptake organs was removed automatically. Additional organs (Liver, Pelvic Lymph Nodes, and Bone) were segmented and used to ensure that uptake was not inaccurately removed from those ROIs.

~ “PARS” (=labellisation)
mais avec des a priori +++

Quantification TMTV automatique

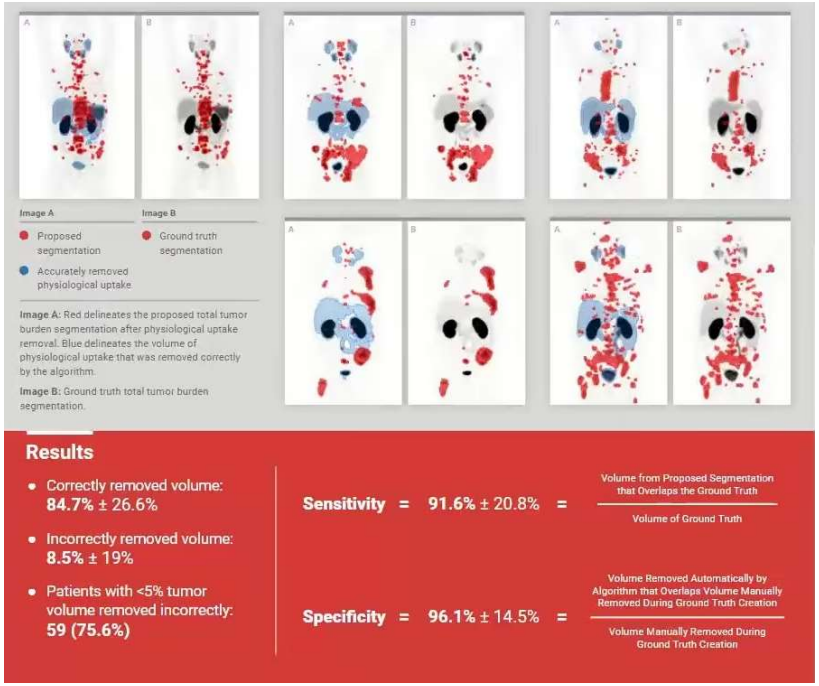

Conclusions: The application of fully automatic organ-based physiological uptake removal results in very similar volumes to those produced by manual editing of TTB volumes. This suggests that minimal additional time would be necessary if used in the clinical workflow. This reduction increases the feasibility of quickly achieving TTB statistics for 68Ga-PSMA-11 PET/CT studies. In future research, we plan to examine the time savings provided by utilizing this automated removal of physiological uptake.

TMTV facile à obtenir → possibilité de tester son utilité

Données manquantes

Handling missing values in machine learning to predict major adverse cardiac events: insights from REFINE SPECT registry

Richard Rios, Robert Miller, Tali Sharir, Andrew Einstein, Mathews Fish, Terrence Ruddy, Philipp Kaufmann, Albert Sinusas, Edward Miller, Timothy Bateman, Sharmila Dorbala, Marcelo Di Carli, Joanna Liang, Damini Dey, Daniel Berman and Piotr Slomka

Journal of Nuclear Medicine May 2021, 62 (supplement 1) 1173;

Objectives: Machine learning (ML) models, integrating imaging and clinical variables, can improve prediction of major adverse cardiovascular events (MACE) in patients undergoing SPECT MPI. However, in clinical practice, some variables required for ML models may be missing for reasons such as incomplete patient questionnaires or a need to interpret stress data in advance. While algorithms exist for handling missing values, it remains unknown how these methods affect patient-specific risk estimates. We evaluated three methods for handling missing values in ML models for patient-specific prediction of MACE risk.

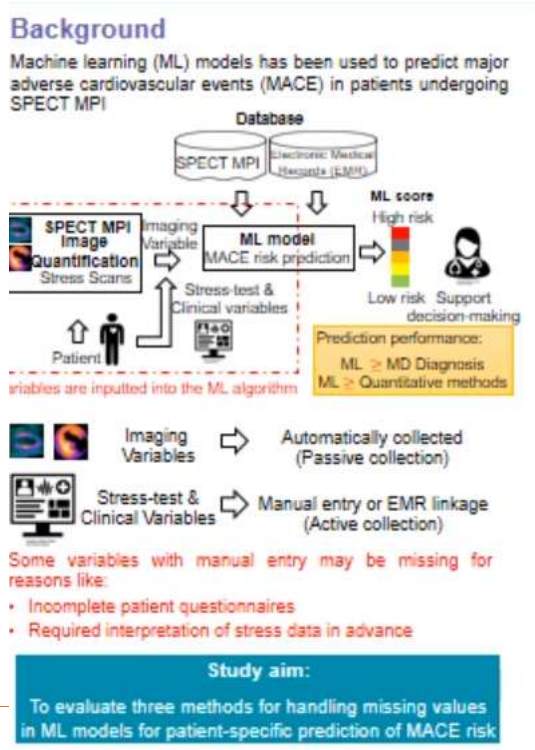

Données manquantes

Methods: This study included 20,414 patients from the multicenter REFINE SPECT registry with images, clinical data, and follow-up for MACE. The average follow-up interval was 4.7±1.5 years. During follow-up, 3,541 patients experienced at least one MACE (3.7% annualized risk): 1,617 deaths, 379 MI, 1,895 revascularizations, and 300 admissions for unstable angina. The dataset included 56 imaging variables and 14 clinical variables. We used extreme gradient boosting (XGBoost) models and evaluated three methods for handling missing values: 1) removal of variables with missing values from the model for MACE prediction (ML-Remove), 2) traditional imputation using the population mean for continuous variables and a distinct missing category for categorical variables (ML-Traditional), and 3) unique category "unknown" imputed for all missing variables, which is the XGBoost's default method for handling the missing variables (ML-Unique). We compared these ML models to the model built with all variables (ML-All). Training and testing was performed with 10-fold cross validation using the registry data. In each of the testing sets (10% of the registry database), we simulated missing clinical data for the variables which are the most difficult to collect and had the highest missing rates in our registry (*indication for test, resting heart rate, body mass index, ECG response, Symptoms, ST deviation, and clinical response to stress)*. ML-Traditional and ML-Unique were tested in a population with all values imputed for those variables. All values were imputed to assess the impact on risk-estimation for an individual patient, where values can either be present or missing. ML-Remove and ML-All were tested with patient specific data. Prediction performance was evaluated using area under the receiver-operating characteristic curve (AUC) and compared with the performance of 4-point scale visual diagnosis and stress total perfusion deficit (TPD) variables.

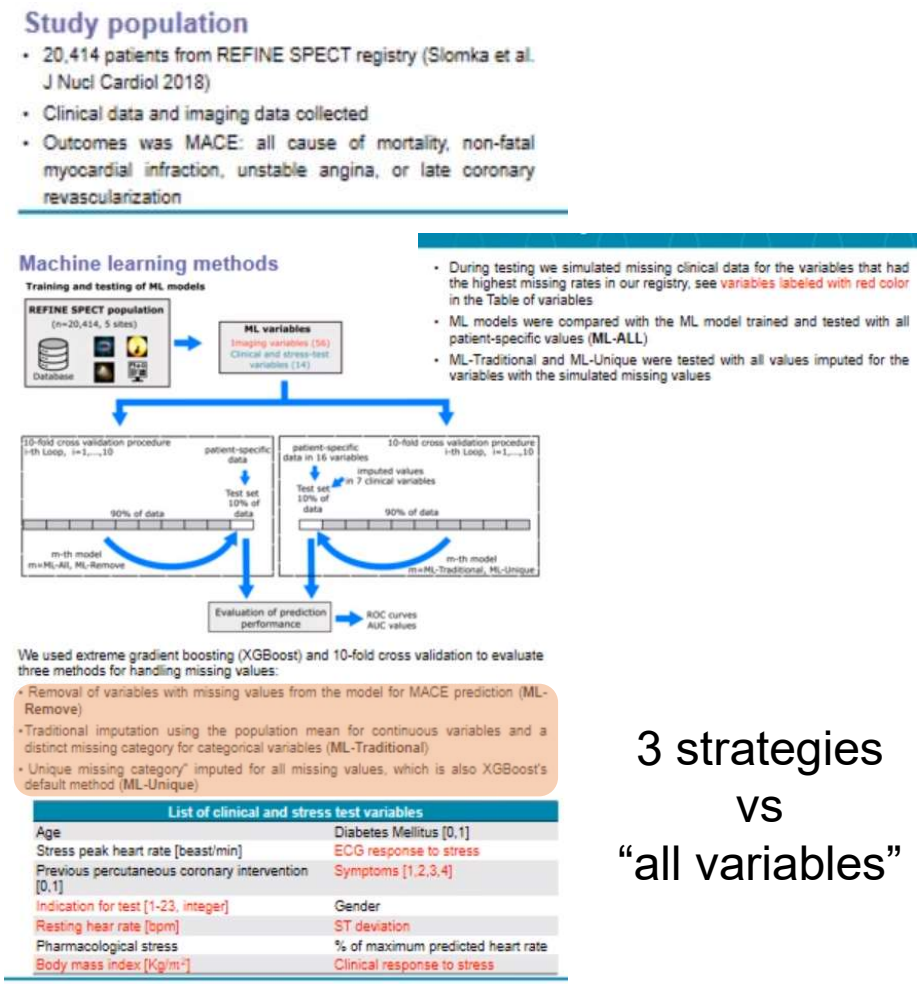

3 strategies
vs
"all variables"

Données manquantes

Results: The best MACE risk prediction was obtained when no variables were missing (ML-All AUC: 0.796, 95% confidence interval [CI]: 0.788 to 0.804). The strategy of removing variables during model training obtained the second best prediction performance followed by the traditional imputation method (ML-Remove AUC: 0.777, 95% CI: 0.769 to 0.785 vs ML-Traditional AUC: 0.768, 95% CI: 0.760 to 0.777; p=NS). ML-Unique obtained lower prognostic accuracy, but this was still higher compared with stress TPD and visual diagnosis alone (ML-Unique AUC: 0.761, 95% CI: 0.753 to 0.770 vs stress TPD AUC: 0.698, 95% CI: 0.688 to 0.708 vs. visual diagnosis AUC: 0.680, 95% CI: 0.671 to 0.690, respectively; p < 0.01 for all). **Conclusions:** In clinical practice, missing values reduce the accuracy of ML models when predicting MACE risk. Our results suggest that removing variables with missing values and retraining the model with fewer variables may yield superior accuracy compared to imputation methods.

Conclusions sont transposables sur d'autres jeux de données ? Effectifs plus faibles ?
Poids des variables manquantes dans le modèle ?

Results

- 20,414 patients were included
- During mean follow-up of 4.7 years, 3541 patients experienced at least one MACE
- The full ML model (ML-All) had the highest accuracy
- The best method for handling missing values was removal of variables with missing values followed by the traditional imputation method

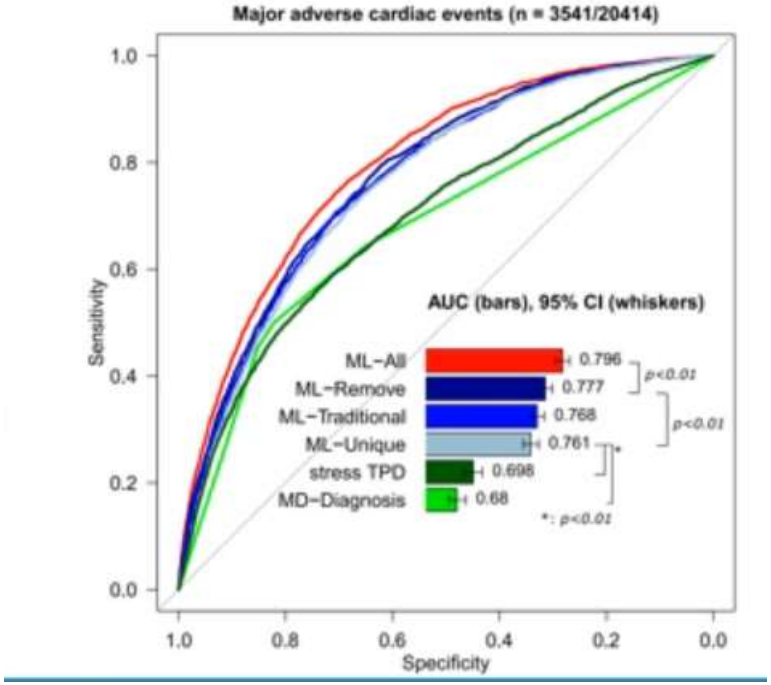

Pays invite : Corrée du Sud

Pays invite : Corrée du Sud

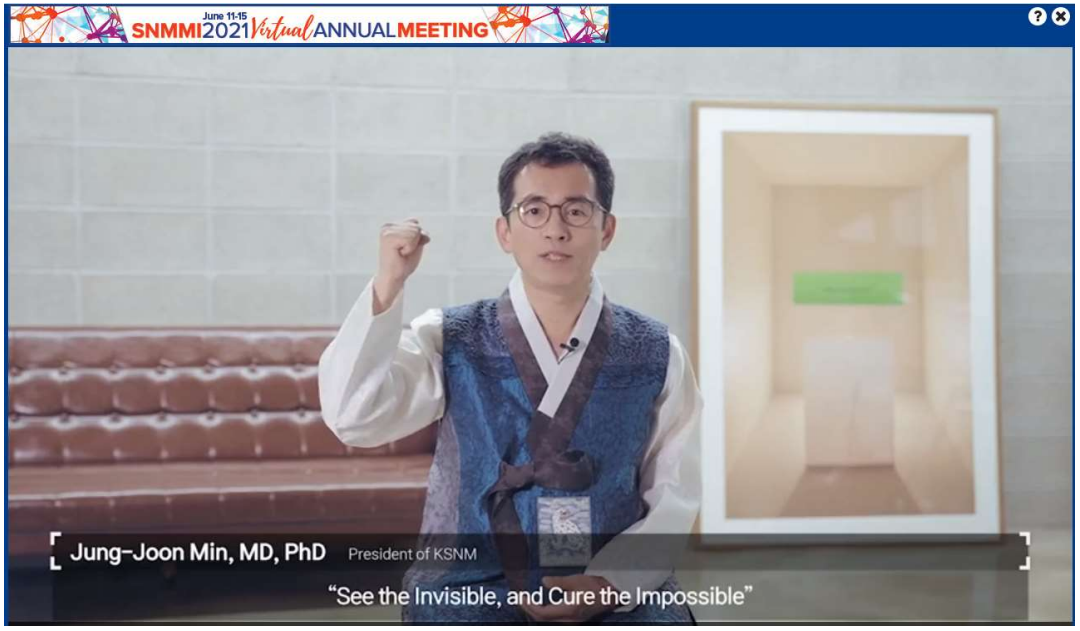

Pays invite : Corrée du Sud

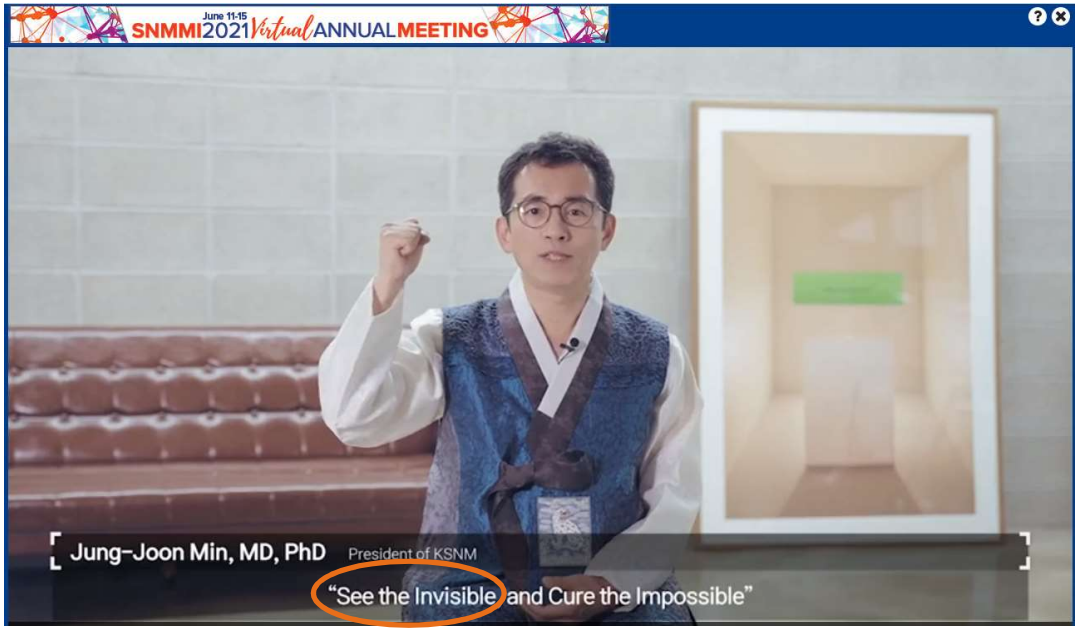

See the invisible: 18F-DASA-23

Initial Clinical Evaluation of [^{18}F]DASA-23, a PET Imaging Tracer for Evaluation of Aberrantly Expressed Pyruvate Kinase M2 in Glioblastoma

Corinne Beinat, Chirag Patel, Tom Haywood, Lewis Naya, Jessa Castillo, Bin Shen, Tarik Massoud, Andrei Iagaru, Guido Davidzon, Lawrence Recht and Sanjiv Gambhir

Journal of Nuclear Medicine May 2021, 62 (supplement 1) 99;

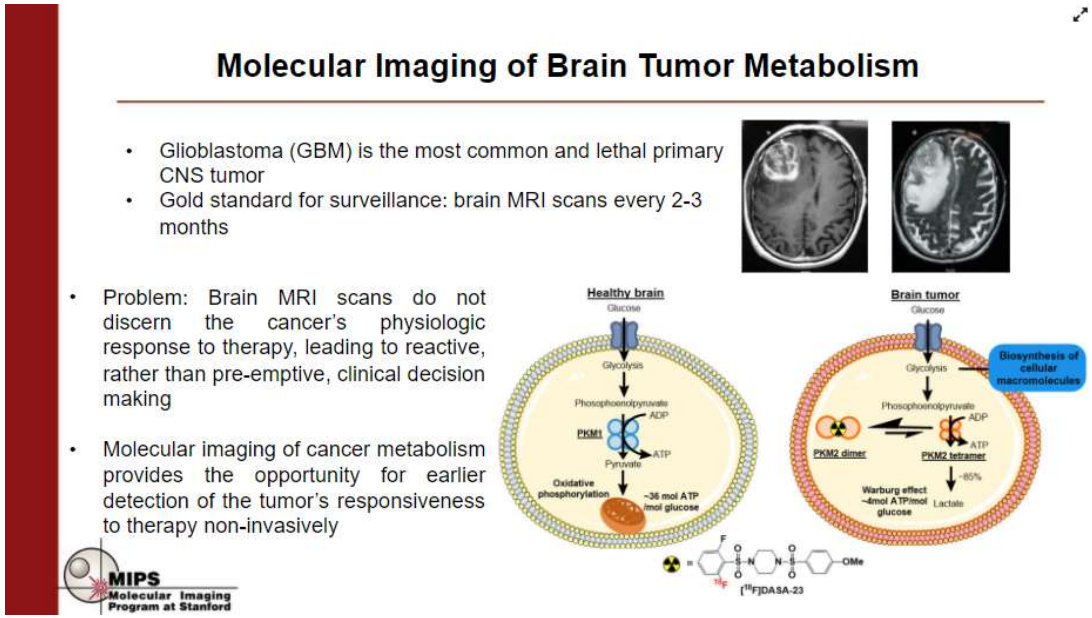

Introduction: Pyruvate kinase M2 (PKM2) catalyzes the final step in glycolysis, a key process of cancer metabolism. PKM2 is preferentially expressed by glioblastoma (GBM) cells with minimal expression in healthy brain, making it an important biomarker of cancer glycolytic re-programming. We describe the translation and initial clinical evaluation of a novel positron emission tomography (PET) tracer 1-((2-fluoro-6-[^{18}F]fluorophenyl)sulfonyl)-4-((4-methoxyphenyl)sulfonyl)piperazine ([^{18}F]DASA-23) in patients with GBM.

Methods: [^{18}F]DASA-23 was synthesized under current Good Manufacturing Practices United States Food and Drug Administration (FDA) oversight with a molar activity of 100.47 ± 29.58 GBq/μmol and radiochemical purity of >95%. In a phase I trial (NCT03539731), we administered

See the invisible: 18F-DASA-23

[18F]DASA-23 Evaluation in Healthy Volunteers – Part 1a

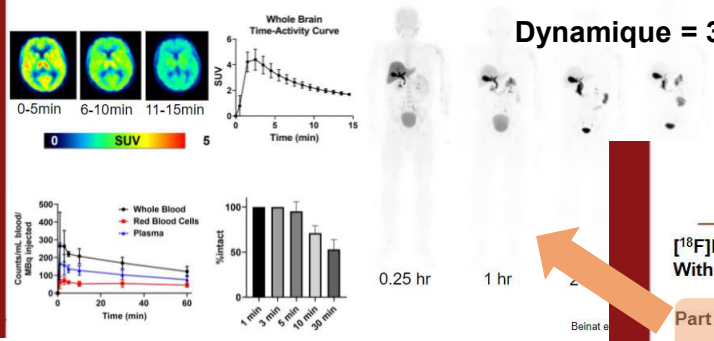

Dynamique = 3h

N = 8 sujets sains

First-In-Human Study of [18F]DASA-23

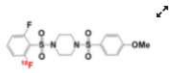

[18F]DASA-23 and PET/MRI Scan in Evaluating Pyruvate Kinase M2 Expression in Patients With Intracranial Tumors or Recurrent Glioblastoma and Healthy Volunteers (NCT03539731)

Part 1a: Determine radiation dosimetry and biodistribution in healthy volunteers. Dynamic brain PET/MRI scan over 15 minutes and 4 vertex-to-toe PET/MRI scans over 3 hours

Part 1b: Brain uptake and distribution of [18F]DASA-23 in healthy volunteers. Dynamic brain PET/MRI scan over 60 minutes

Part 2: [18F]DASA-23 uptake in intracranial tumor patients. Dynamic brain PET/MRI over 60 minutes

Part 3: Response assessment of glioblastoma patients using [18F]DASA-23 PET/MRI pre- and post-therapy. Dynamic brain PET/MRI scan over 60 minutes

MIPS Molecular Imaging Program at Stanford

See the invisible: 18F-DASA-23

Dynamique = 60 min

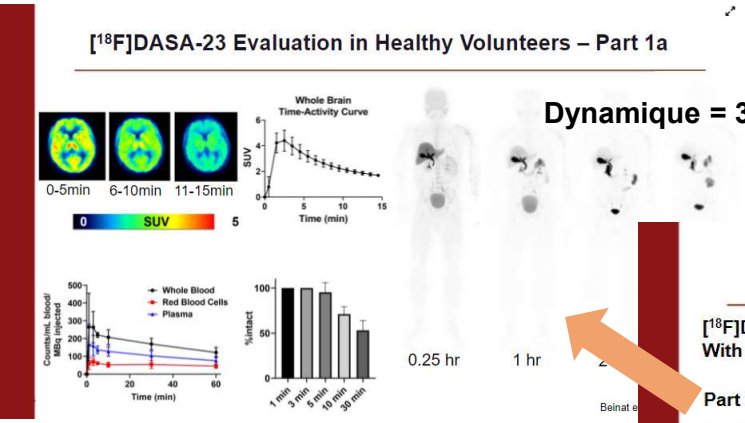

N = 8 sujets sains

First-In-Human Study of [18F]DASA-23

[18F]DASA-23 and PET/MRI Scan in Evaluating Pyruvate Kinase M2 Expression in Patients With Intracranial Tumors or Recurrent Glioblastoma and Healthy Volunteers (NCT03539731)

Part 1a: Determine radiation dosimetry and biodistribution in healthy volunteers. Dynamic brain PET/MRI scan over 15 minutes and 4 vertex-to-toe PET/MRI scans over 3 hours

Part 1b: Brain uptake and distribution of [18F]DASA-23 in healthy volunteers. Dynamic brain PET/MRI scan over 60 minutes

Part 2: [18F]DASA-23 uptake in intracranial tumor patients. Dynamic brain PET/MRI over 60 minutes

Part 3: Response assessment of glioblastoma patients using [18F]DASA-23 PET/MRI pre- and post-therapy. Dynamic brain PET/MRI scan over 60 minutes

MIPS Molecular Imaging Program at Stanford

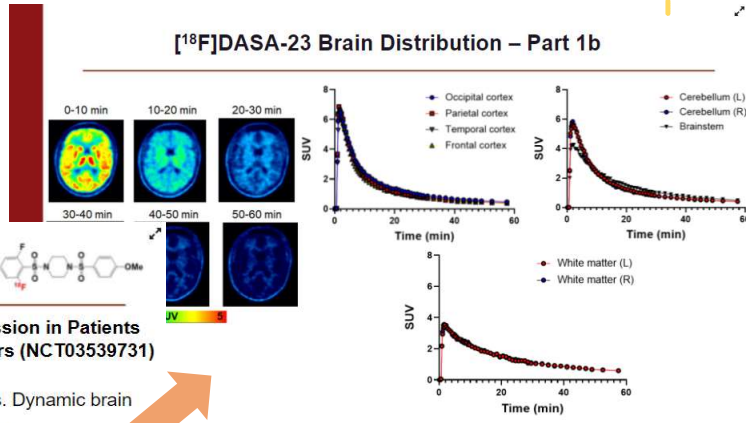

See the invisible: 18F-DASA-23

Dynamique = 60 min

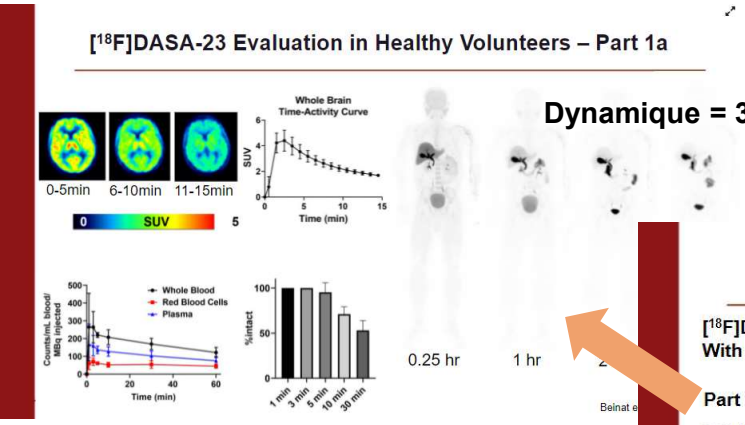

Dynamique = 3h

N = 8 sujets sains

First-In-Human Study of [18F]DASA-23

[18F]DASA-23 and PET/MRI Scan in Evaluating Pyruvate Kinase M2 Expression in Patients With Intracranial Tumors or Recurrent Glioblastoma and Healthy Volunteers (NCT03539731)

Part 1a: Determine radiation dosimetry and biodistribution in healthy volunteers. Dynamic brain PET/MRI scan over 15 minutes and 4 vertex-to-toe PET/MRI scans over 3 hours

Part 1b: Brain uptake and distribution of [18F]DASA-23 in healthy volunteers. Dynamic brain PET/MRI scan over 60 minutes

Part 2: [18F]DASA-23 uptake in intracranial tumor patients. Dynamic brain PET/MRI over 60 minutes

Part 3: Response assessment of glioblastoma patients using [18F]DASA-23 PET/MRI pre- and post-therapy. Dynamic brain PET/MRI scan over 60 minutes

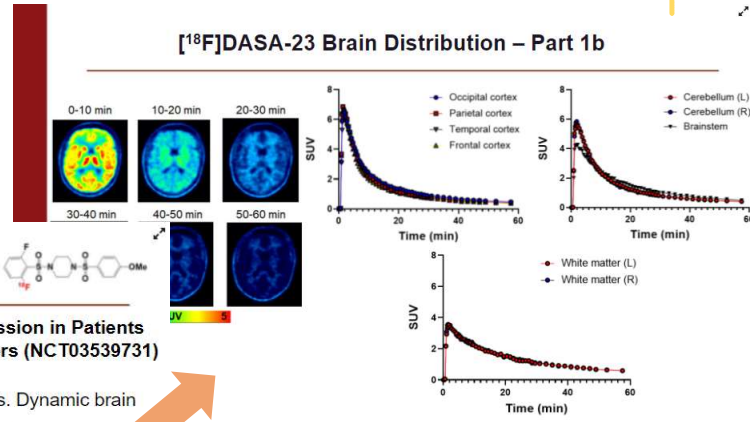

N = 10 patients avec un GBM

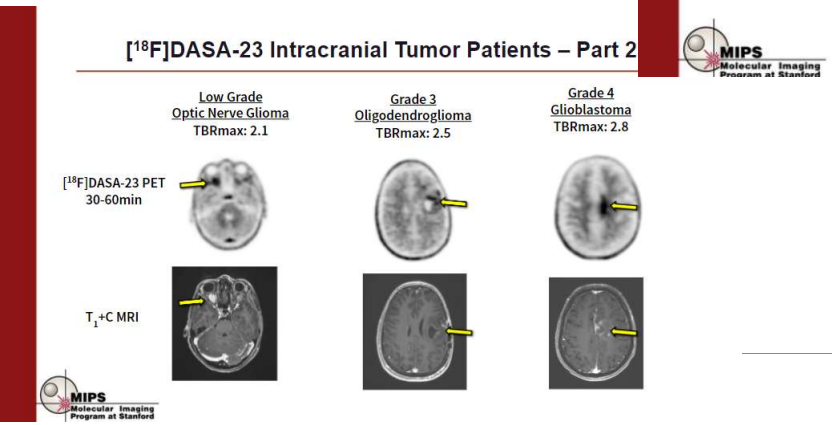

See the invisible: 18F-DASA-23

Dynamique = 60 min

Dynamique = 3h

[18F]DASA-23 Evaluation in Healthy Volunteers – Part 1a

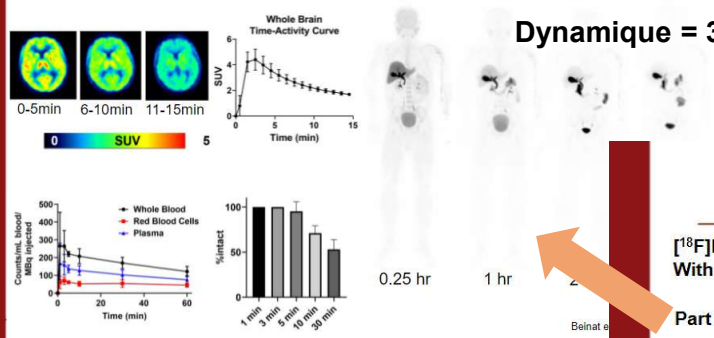

N = 8 sujets sains

First-In-Human Study of [18F]DASA-23

[18F]DASA-23 and PET/MRI Scan in Evaluating Pyruvate Kinase M2 Expression in Patients With Intracranial Tumors or Recurrent Glioblastoma and Healthy Volunteers (NCT03539731)

Part 1a: Determine radiation dosimetry and biodistribution in healthy volunteers. Dynamic brain PET/MRI scan over 15 minutes and 4 vertex-to-toe PET/MRI scans over 3 hours

Part 1b: Brain uptake and distribution of [18F]DASA-23 in healthy volunteers. Dynamic brain PET/MRI scan over 60 minutes

Part 2: [18F]DASA-23 uptake in intracranial tumor patients. Dynamic brain PET/MRI over 60 minutes

Part 3: Response assessment of glioblastoma patients using [18F]DASA-23 PET/MRI pre- and post-therapy. Dynamic brain PET/MRI scan over 60 minutes

[18F]DASA-23 Brain Distribution – Part 1b

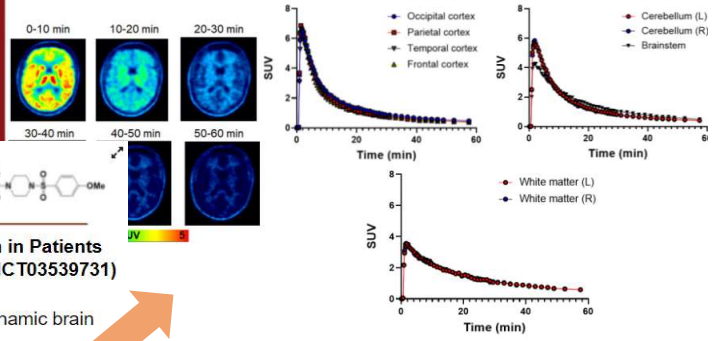

N = 10 patients avec un GBM

[18F]DASA-23 Intracranial Tumor Patients – Part 2

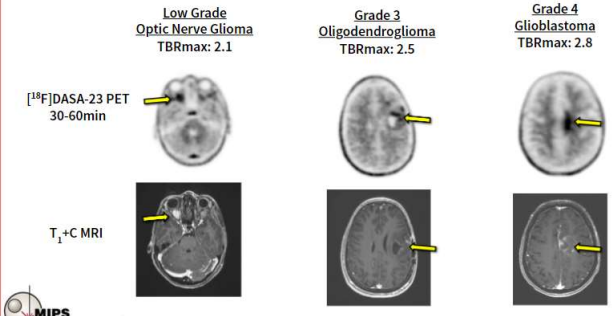

eriod (Fig. 1b). In patients with intracranial malignancies, [18F]DASA-23 successfully visualized ontrast-enhancing tumors with a trend towards increasing uptake with increasing tumor grade (Fig. c). In a GBM patient, [18F]DASA-23 SUVmean and SUVmax were 2.0 and 2.2, respectively. The bsence of PKM2 within healthy brain resulted in a high tumor-to-brain ratio (TBR) of 2.5 and a

[18F]DASA-23 Response Assessment – Part 3

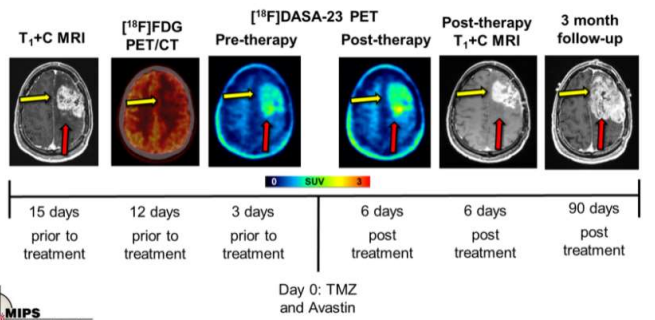

See the invisible: 18F-DASA-23

Conclusions and Ongoing Work

- [^{18}F]DASA-23 is a new radiotracer for PKM2 and is approved for evaluation in healthy volunteers and patients
- [^{18}F]DASA-23 is safe to use in humans with no adverse events or changes in blood labs
- We are recruiting patients to evaluate the ability of [^{18}F]DASA-23 to detect early therapeutic response in newly diagnosed and recurrent glioblastoma (NCT03539731)
- Other studies involving this tracer include:

Tumor treating fields (TTFields) impairs aberrant glycolysis in glioblastoma as evaluated by [^{18}F]DASA-23
Neoplasia, 2021

Evaluation of Glycolytic Response to Multiple Classes of Anti-glioblastoma Drugs by Noninvasive Measurement of Pyruvate Kinase M2 Using [^{18}F]DASA-23
Mol Imag Biol, 2019

Positron emission tomography reporter gene strategy for use in the central nervous system
PNAS, 2019

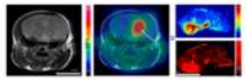

MIPS Molecular Imaging Program at Stanford

PRIMARY OBJECTIVES:

I. Determine whether the fluorine F 18 DASA-23 ([18F]DASA 23) PET scan signal change from pre-therapy to one week after initiation of therapy can predict the tumor's responsiveness to therapy and 6 month progression free survival (PFS6), in suspected recurrent glioblastoma.

Study Type :	Interventional (Clinical Trial)
Estimated Enrollment :	25 participants
Allocation:	Non-Randomized
Intervention Model:	Sequential Assignment
Masking:	None (Open Label)
Primary Purpose:	Diagnostic
Official Title:	A Phase I Study of [18F]DASA-23 as a PET Tracer for Evaluating Pyruvate Kinase M2 (PKM2) Expression in Healthy Volunteers and in Patients With Intracranial Tumors
Actual Study Start Date :	April 23, 2018
Estimated Primary Completion Date :	July 30, 2022
Estimated Study Completion Date :	December 30, 2022

LITO

Pays invite : Corrée du Sud

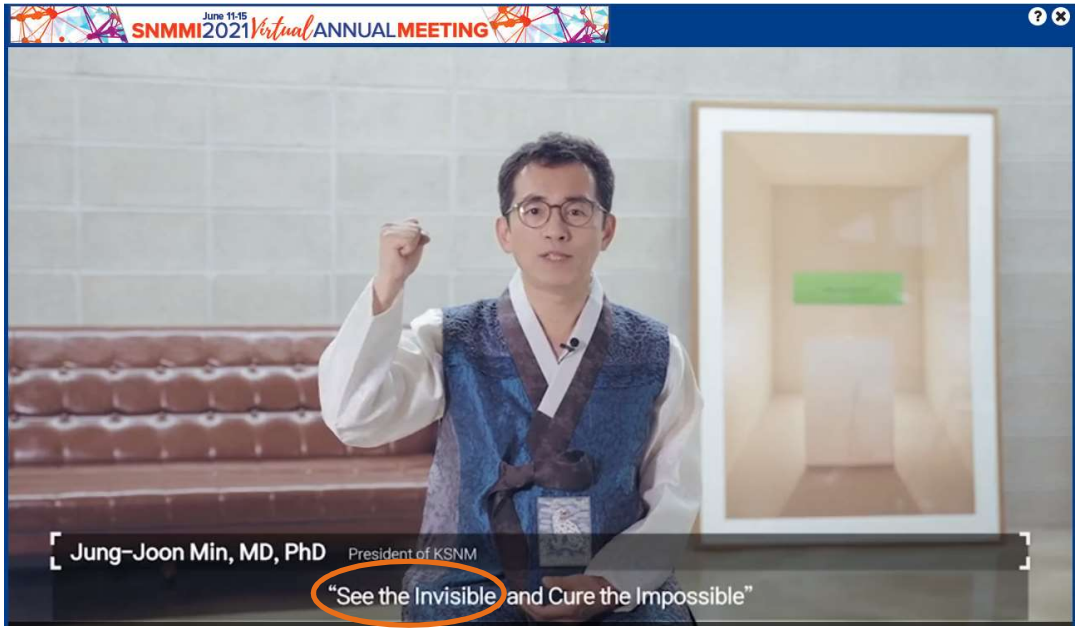

See the invisible: FAPI+++

More on FAPI

SNMMI 2019 – Image of the Year

- Meanwhile
  - Numerous case reports and small clinical studies
    - Utility for diagnosis, staging, RT planning, change in pt. management
    - Lung, pancreas, gastric, lower GI, HNC incl. ACC and NPC, sarcoma, peritoneal carcinomatosis
  - Non-cancer
    - ECD, thyroiditis, benign pancreas lesions, pulmonary fibrosis, FD, solitary fibrous tumor, elastofibroma…
    - Post-MI fibroblast activation

Tumor Microenvironment – CAFs and FAP

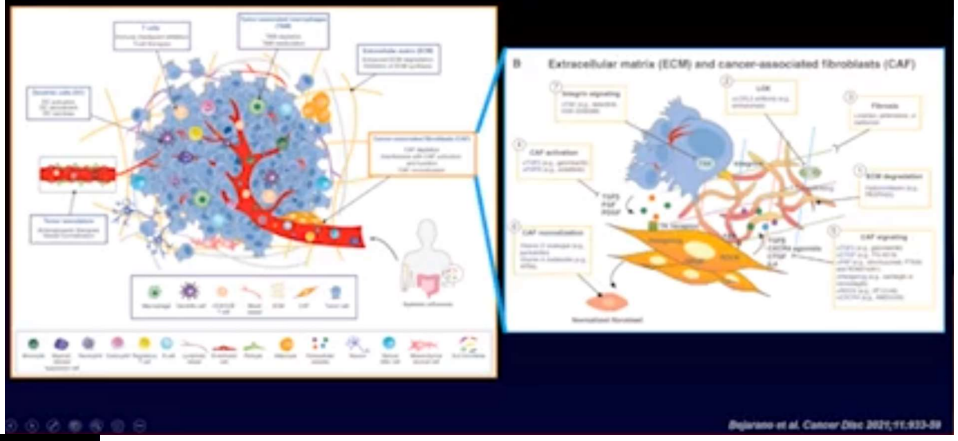

CAFs and FAP

Cancer Associated Fibroblasts	Fibroblast Activating Protein

• Subpopulation of activated fibroblasts in the TME
• Relevant for
  ▪ Angiogenesis
  ▪ Cell migration and metastasis
  ▪ Immune suppression
  ▪ Resistance to chemotherapy, anti-androgens
• Actions
  ▪ Secretion of growth factors, chemokines
  ▪ Remodeling of ECM
  ▪ Cooperative metabolism w/cancer cells
	• Only expressed on *activated* fibroblasts
	• Transmembrane glycoprotein
	• Enzymatic activity as peptidase
	• Various physiologic roles in normal development
	• Prognostic marker in cancer
	• Can be targeted with AB, AB-drug-conjugates, immunocytokines, CAR T-cells, activatable prodrugs, enzyme inhibitors…
	  ▪ Radiolabeled FAPI for theranostics
	  ▪ Poss. synergistic with immunotherapies

institut Curie

FAP = *Fibroblast Activation Protein*
Très exprimée dans le stroma tumoral

See the invisible: FAPI+++

Validation of FAPi PET biodistribution by immunohistochemistry in patients with solid cancers: a prospective exploratory imaging study

Christine Mona, Matthias Benz, Firas Hikmat, Tristan Grogan, Katharina Lueckerath, Ali Aria Razmaria, Rana Riahi, Roger Slavik, Mark Grigis, Giuseppe Carlucci, Kimberly Kelly, Johannes Czernin, David Dawson and Jeremie Calais

Journal of Nuclear Medicine May 2021, 62 (supplement 1) 1000;

Introduction: Fibroblast activation protein (FAP)-expressing cancer associated fibroblasts (CAFs), a major component of tumor stroma, confer treatment resistance, promote local progression, metastasis and immunosuppression. Because FAP is selectively expressed in the tumor stroma of many cancers, radiolabeled small molecule ligands targeting FAP are being explored for their use as pan-cancer theranostic agents. The objective was to define the incidence and degree of FAP expression by immunohistochemistry (IHC) across various cancers using Tissue Microarrays (TMAs) and to explore whether gallium-68 FAPi-46 PET image biodistribution faithfully reflects tumor FAP expression from resected tumor and non-tumor specimens.

See the invisible: FAPI+++

Methods: This study was a prospective, exploratory, open-label, single-center imaging trial in cancer patients conducted in 2020. Referred volunteer **p**atients scheduled to undergo surgical resection of the primary tumor and/or metastases were eligible. Patients underwent one whole body 68Ga-FAPI-46 PET/CT scan. Subsequently, patients underwent surgical resection of the primary tumor and/or metastasis. The **Outcome Measure was the** Correlation of 68Ga-FAPI-46 PET maximum standardized uptake value (SUVmax) with FAP IHC score in cancer and non-cancer tissue. **Trial Registration**: ClinicalTrials.gov Identifier: NCT04147494.

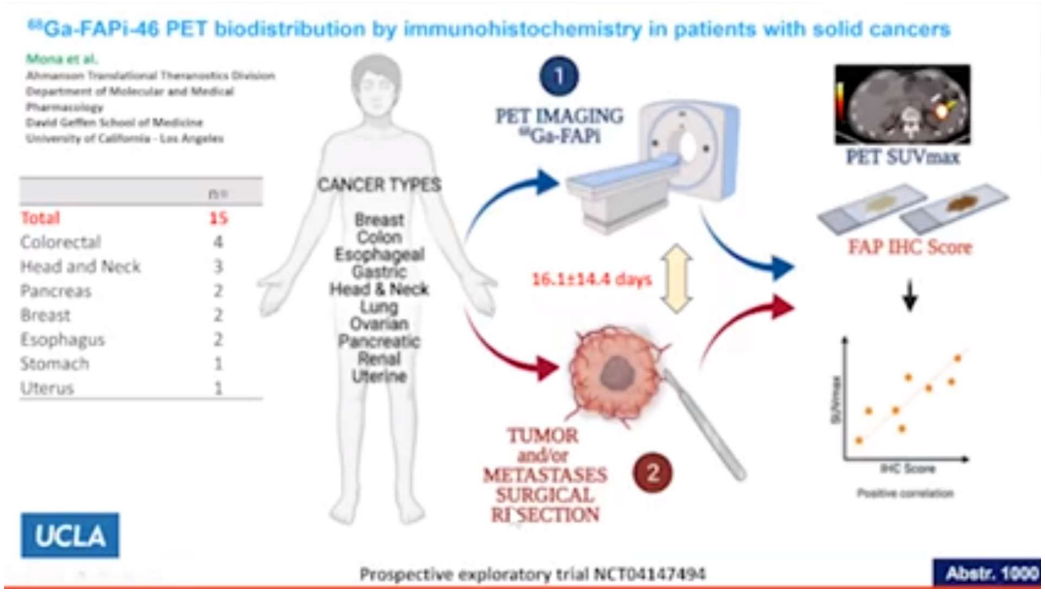

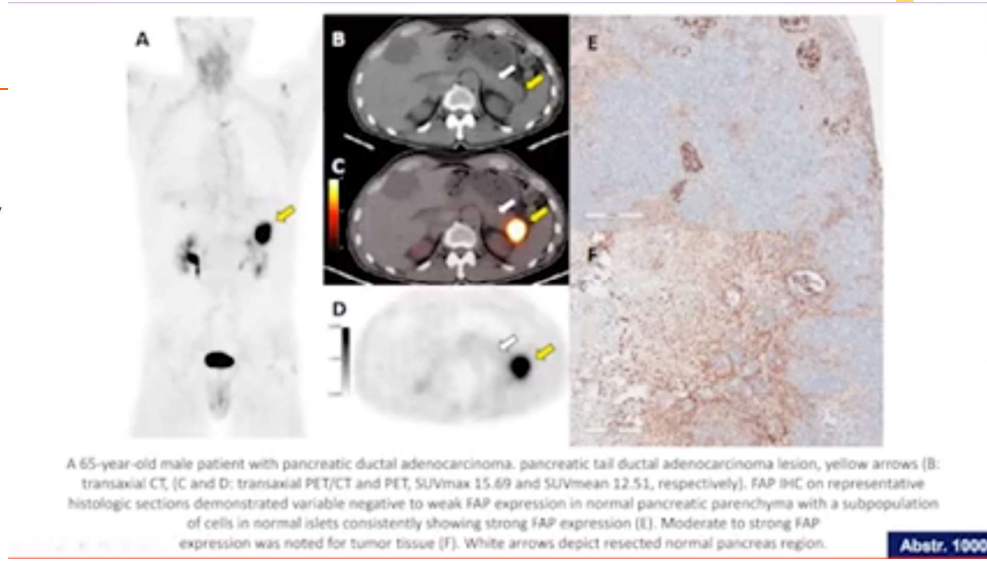

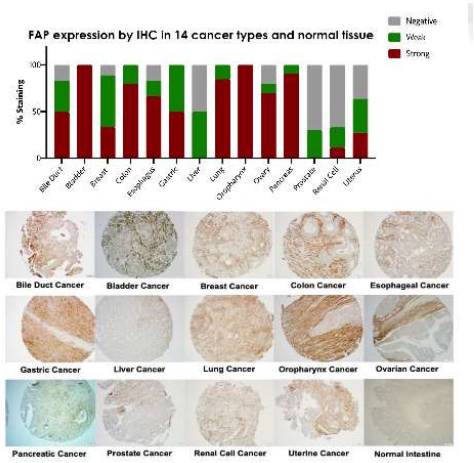

See the invisible: FAPI+++

Results: The incidence of FAP expression in TMAs from 14 cancers ranged from 25 to 100% (mean 76.6± 25.3). 15 patients with the following cancer types were included: colorectal (n=4), head and neck (n=3), pancreas (n=2), breast (n=2), stomach (n=1), esophagus (n=2) and uterus (n=1). All 15 patients subsequently underwent surgery after the scan with a mean time interval of16.1 ± 14.4 days (range 1 - 50 days). Tumor resection was not attempted in 2 patients because unresectable. FAPI SUVmax and IHC score were higher in cancer tissue than in normal tissue: mean FAPI SUVmax 7.4±4.6 (range 1.5-15.9) vs 1.6±1.2 (range 0.4-5.1), (p<0.001) and mean FAP IHC score 2.38±0.65 vs 0.54±0.66 (p<0.001), respectively. The FAP IHC score was positively correlated with FAPI SUVmax (pairwise p=0.001, repeated measures correlations r=0.85 (95% CI 0.53-0.95), p<0.001).

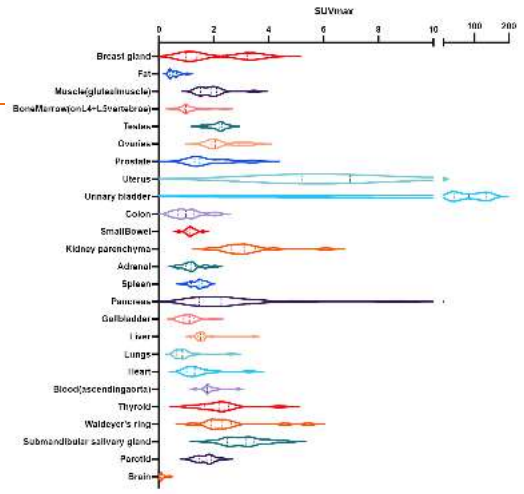

^{68}Ga-FAPi-46 uptake in normal organs

15 patients/7 types de cancer

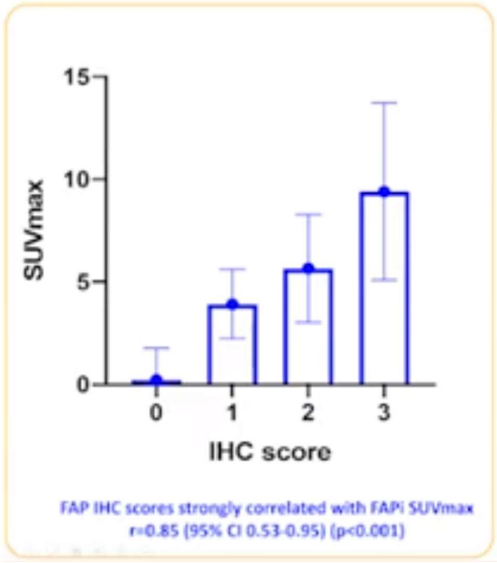

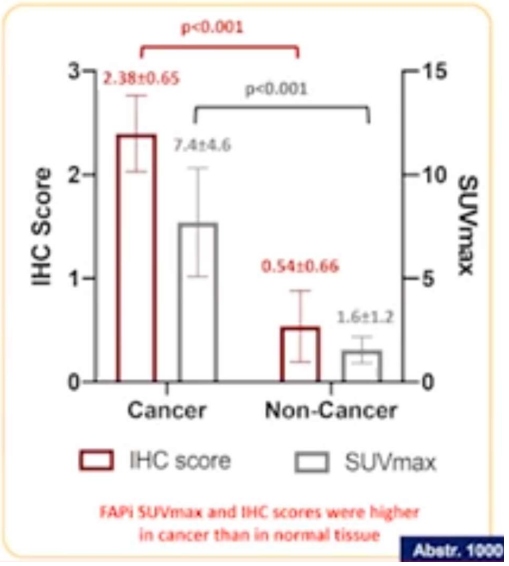

See the invisible: FAPI+++

Conclusions: The ^{68}Ga-FAPi-46 PET biodistribution across multiple cancers reflects FAP expression as determined by IHC. This translational validation paves the way for large scale prospective trials on the use of ^{68}Ga-FAPi-46 PET/CT as a biomarker and stratification tool for FAP-targeted therapies.

CONCLUSION:

- **FAPI uptake** tends to be **significantly higher in cancer** tissues vs. non-cancer tissues
- **^{68}Ga-FAPi-46 PET biodistribution** across multiple cancers **strongly correlates with fibroblast activation protein tissue expression** as measured by immunohistochemistry
- Staining intensity was higher in stromal areas within and immediately adjacent to the malignant epithelial compartment of tumors.
- **FAP staining** was exclusively **confined to the tumor-associated stromal compartment** in most patients
- The highest FAP IHC scores were observed in pancreatic, esophageal and breast cancer.

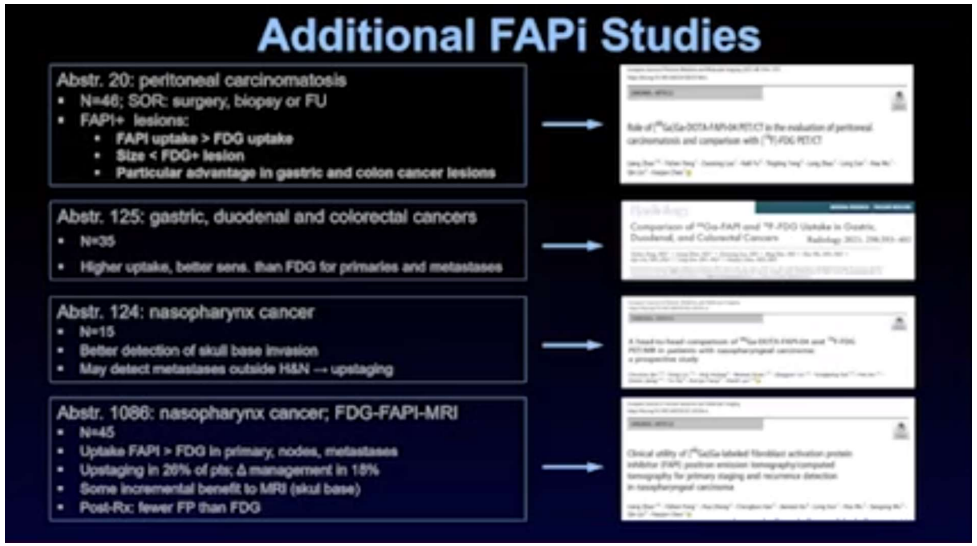

Pays invite : Corrée du Sud

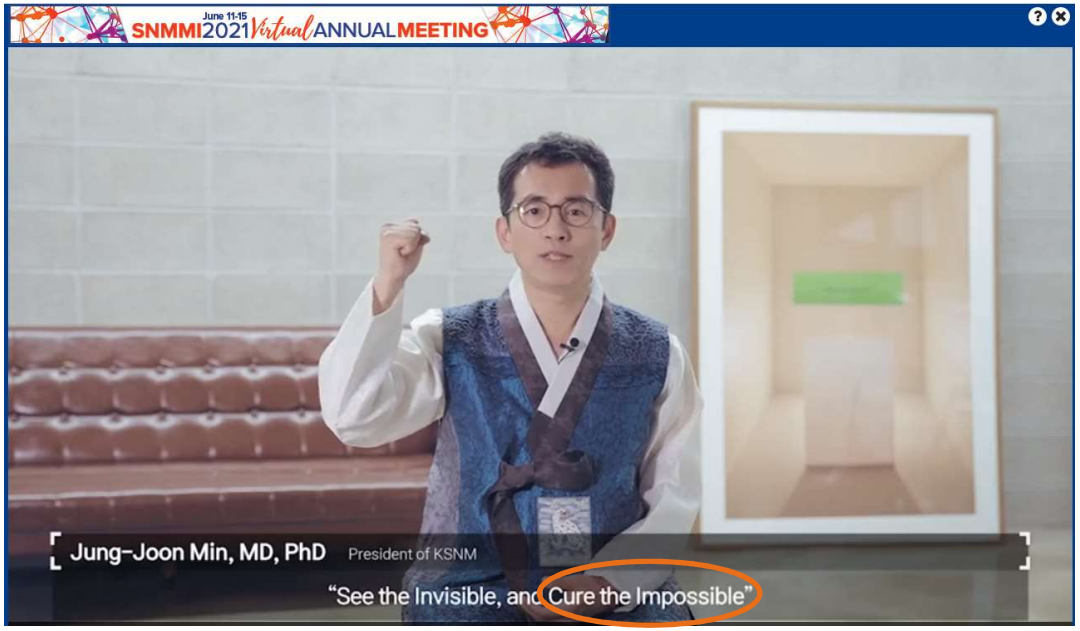

Cure the impossible: TheraP

^{177}Lu-PSMA-617 versus Cabazitaxel in Metastatic Castration-Resistant Prostate Cancer: a randomised, open-label, phase 2 trial (TheraP)

Michael Hofman, Louise Emmett, Amir Iravani, Shahneen Sandhu, Anthony Joshua, David Pattison, Jeffrey Goh, Ian Kirkwood, Thean Hsiang Tan, Roslyn Francis, Siobhan Ng, Natalie Rutherford, Craig Gedye, Andrew Scott, Sze-Ting Lee, Andrew Weickhardt, Shakher Ramdave, Edmond Kwan, Arun Azad, William Macdonald, Andrew Redfern, Alison Zhang, Martin Stockler, Andrew Martin and Ian Davis

Journal of Nuclear Medicine May 2021, 62 (supplement 1) 1703;

Objectives: ^{177}Lu-PSMA-617 is a radiolabelled small molecule that delivers β-radiation to cells expressing prostate specific membrane antigen (PSMA), with promising activity and safety in metastatic castration-resistant prostate cancer (mCRPC). We compared ^{177}Lu-PSMA-617 and cabazitaxel in a randomised phase 2 trial.

Methods: Men with mCRPC progressing after docetaxel with high PSMA tumour-expression were randomized to ^{177}Lu-PSMA-617 (6-8.5 GBq intravenously 6 weekly up to 6 cycles) vs cabazitaxel (20 mg/m^2 intravenously 3 weekly up to 10 cycles) at 11-sites in Australia. The primary endpoint was prostate specific antigen (PSA) response rate defined by ≥50% reduction (PSA50-RR). Secondary endpoints included progression-free survival (PFS) (PSA and radiographic PFS), objective response rate (ORR) (RECIST 1.1), adverse events (CTCAE v4.03), patient-reported outcomes (PROs) (EORTC QLQ-C30, PDF), and overall survival (OS). This trial is registered in ClinicalTrials.gov, NCT03392428.

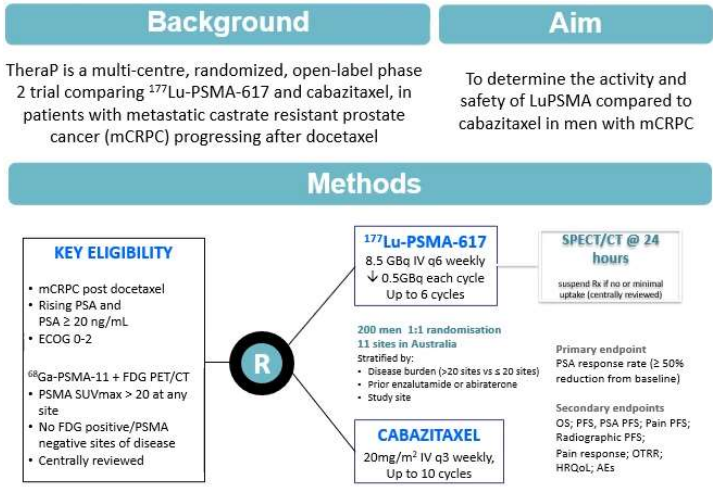

Cure the impossible: TheraP

Results: 200 of 291 men identified as eligible on PET imaging were randomised to ^{177}Lu-PSMA-617 (N=99) or cabazitaxel (N=101). 91% had received prior androgen receptor-directed therapy (ARDT). PSA50-RR was significantly higher in those assigned ^{177}Lu-PSMA-617 versus cabazitaxel (66% [95%CI,56-75%] vs 37% [95%CI,27-46%]; P<0.001). PFS was significantly longer in those assigned ^{177}Lu-PSMA-617 than cabazitaxel (rates at 1yr 19% [95%CI,12-27%] vs 3% [95%CI,1-9%], hazard ratio (HR) 0·63 [95%CI,0.46-0.86; P=0.003). ORR in 78 men with measurable disease was significantly higher with ^{177}Lu-PSMA-617 than cabazitaxel (49% vs 24%, RR 2.12; P=0.026). Follow-up remains immature for OS. Grade 3-4 adverse events occurred in 32/98 (33%) with ^{177}Lu-PSMA-617 vs 45/85 (55%) with cabazitaxel. Overall quality-of-life and health status were similar, with significantly better outcomes for multiple PRO domains including diarrhoea, fatigue, social functioning, insomnia, hair loss, skin rash and sore hands/feet with ^{177}Lu-PSMA-617.

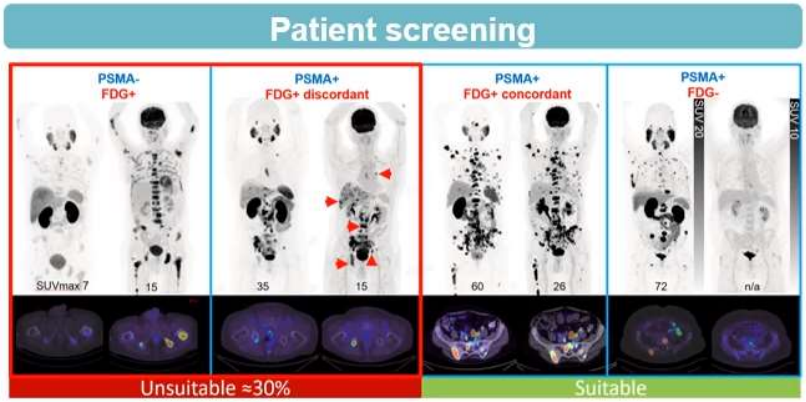

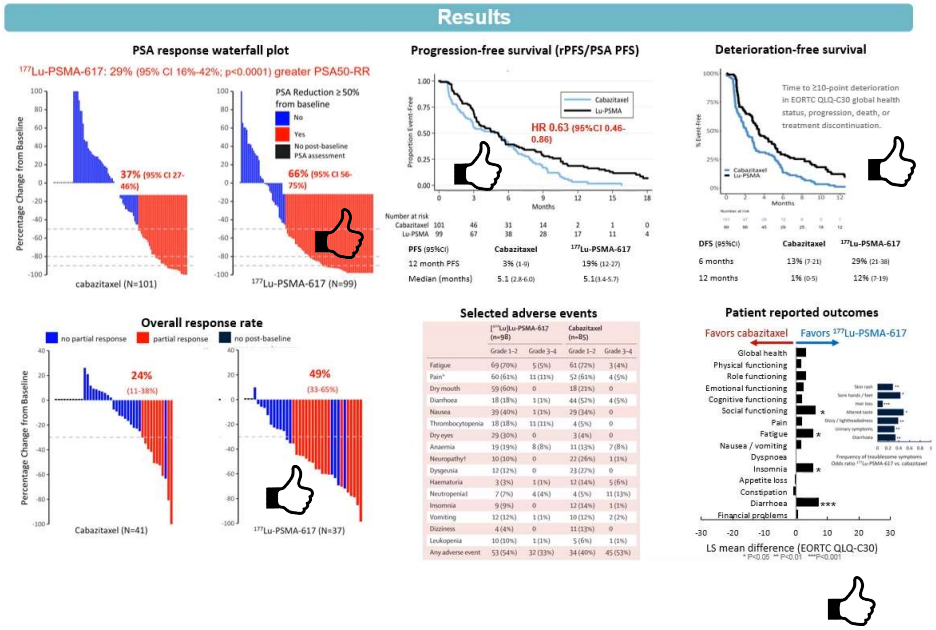

Conclusions: ^{177}Lu-PSMA-617 compared to cabazitaxel in men with mCRPC led to significantly higher PSA and ORR response rates, longer PFS, less grade 3 or 4 adverse events and significant improvements in several PRO domains.

Image de l’année

Altered regional cerebral function and its association with cognitive impairment in COVID-19: A prospective FDG PET study

Ganna Blazhenets, Nils Schroeter, Tobias Bormann, Johannes Thurow, Dirk Wagner, Lars Frings, Cornelius Weiller, Andrea Dressing, Jonas Hosp and Philipp Meyer

Journal of Nuclear Medicine May 2021, 62 (supplement 1) 41;

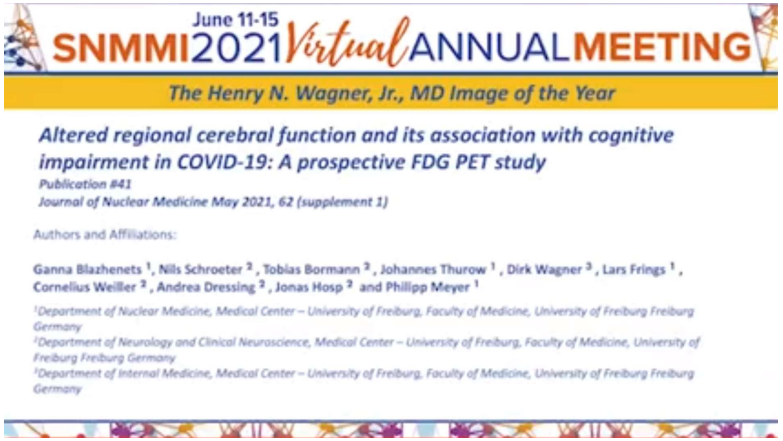

June 11-15
SNMMI2021 Virtual ANNUAL MEETING

The Henry N. Wagner, Jr., MD Image of the Year

Altered regional cerebral function and its association with cognitive impairment in COVID-19: A prospective FDG PET study

Publication #41
Journal of Nuclear Medicine May 2021, 62 (supplement 1)

Authors and Affiliations:

Ganna Blazhenets [1], Nils Schroeter [2], Tobias Bormann [2], Johannes Thurow [1], Dirk Wagner [3], Lars Frings [1], Cornelius Weiller [2], Andrea Dressing [2], Jonas Hosp [2] and Philipp Meyer [1]

[1]Department of Nuclear Medicine, Medical Center – University of Freiburg, Faculty of Medicine, University of Freiburg Freiburg Germany
[2]Department of Neurology and Clinical Neuroscience, Medical Center – University of Freiburg, Faculty of Medicine, University of Freiburg Freiburg Germany
[3]Department of Internal Medicine, Medical Center – University of Freiburg, Faculty of Medicine, University of Freiburg Freiburg Germany

Conclusions: Neocortical dysfunction accompanied by cognitive impairment was detected in two-thirds of inpatients with subacute COVID-19. Although a significant recovery of regional neuronal function and cognition can be clearly stated, residuals are still measurable in some patients six month after manifestation of COVID-19. In consequence, post-COVID-19 patients with persistent cognitive complaints should be presented to a neurologist and possibly allocated to cognitive rehabilitation programs.

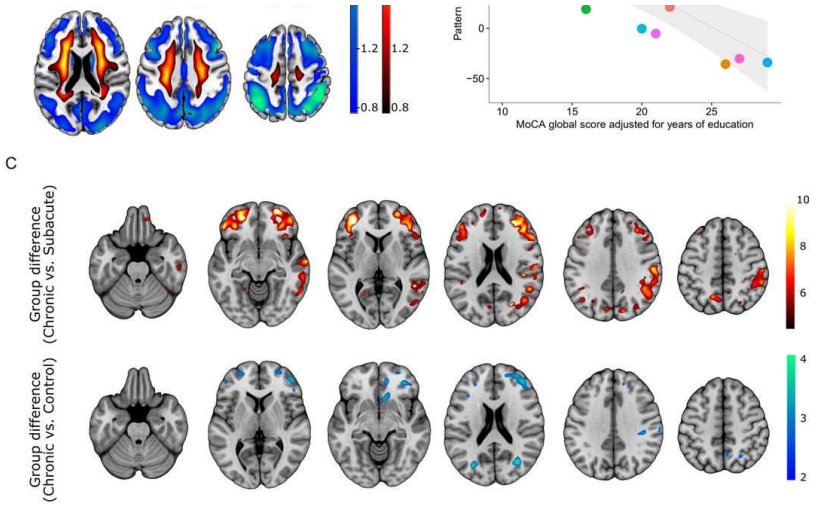

A: COVID-19-related spatial covariance pattern of cerebral glucose metabolism overlaid onto an MRI template. Voxels with negative region weights are color-coded in cool colors, and regions with positive region weights in hot colors. **B:** Association between the expression of COVID-19-related covariance pattern and the Montreal Cognitive Assessment (MoCA) score adjusted for years of education. Each dot represents an individual patient’s data (shaded grey area: 95%-confidence interval). **C:** Results of a statistical parametric mapping analysis. Upper row illustrates regions that show significant increases of normalized FDG uptake in COVID-19 patients at the chronic compared to the subacute stage (paired t test, $p < 0.01$, false discovery rate-corrected). Bottom row depicts regions that still show significant decreases of normalized FDG uptake in COVID-19 patients at the chronic stage compared to the age-matched control cohort at an exploratory statistical threshold (two-sample t test, $p < 0.005$). SPM T values are color-coded and overlaid onto an MRI template. Images are presented in neurologic orientation, i.e., left image side corresponds to patients' left body side; numbers denote axial (Z) position in mm.


Save the Date
June 11-14
SNMMI 2022
ANNUAL MEETING
Vancouver Convention Centre ▸ Vancouver, British Columbia Canad


Save the Date
June 11-14
SNMMI 2022
ANNUAL MEETING
Vancouver Convention Centre ▸ Vancouver, British Columbia Canad